Int. J. Heat Mass Transfer. Vol. 6, pp. 815–832. Pergamon Press 1963. Printed in Great Britain.

DISSOCIATED LAMINAR BOUNDARY LAYER FLOWS OVER SURFACES WITH ARBITRARY CONTINUOUS DISTRIBUTIONS OF CATALYCITY

G. R. INGER*

Aerospace Corporation, Los Angeles 45, California

(*Received* 6 *December* 1962 *and in revised form* 18 *January* 1963)

Abstract—This paper studies several new types of exact series solutions to the diffusion equation for chemically-frozen, dissociated, laminar boundary-layer flows around bodies with arbitrary continuous distributions of a first-order atom recombination rate along the surface. Plate, wedge, and cone flows are considered. The analysis extends the theory of Chambré and Acrivos for constant surface catalytic efficiency and temperature to the case wherein the surface Damkohler number varies as any power of the distance or is distributed as any polynomial involving integer or fractional positive powers of the distance. Furthermore, by imposing the approximation of local similarity in the velocity profile, the resulting solutions are also applied with good accuracy to highly-cooled blunt-nosed bodies in hypersonic flow.

An approximate method of solution is also developed which provides an extremely simple closed-form representation of the exact series solutions throughout the entire flow field by means of a local nonlinear extrapolation of the leading term in the series. It is shown by several examples that this technique yields very accurate results for surface atom concentration, diffusion flux, and heat-transfer distributions for a variety of streamwise variations in the wall catalycity.

NOMENCLATURE

a, exponent for power-law inviscid flow (16);

A_n, A_n', series coefficients (22) and (32);

a_2, a_4, a_6, coefficients in blunt body flow solution (37);

b, exponent for power-law inviscid flow (16);

B_κ, coefficients in series representation Damkohler number distribution (27);

B_λ, B_λ', coefficients in power-law Damkohler number distribution [(31), Fig. 3];

B_s, stagnation point velocity gradient $[(du_e/dx)_s]$;

b_2, b_4, b_6, coefficients in blunt body solution (38);

C, Chapman–Rubesin parameter $(\rho\mu/\rho_e\mu_e)$;

C_P, constant pressure specific heat;

$\bar{C}_P$, average specific heat of mixture;

c_2, c_4, c_6, coefficients in blunt body flow solution (40);

d, exponent in power law distribution of K_w/μ_w, (34) and (38);

g, h/h_e;

h, total temperature-sensitive enthalpy $\left(\bar{C}_P T + \frac{u^2}{2}\right)$;

h_D, specific dissociation energy;

$I(\eta)$, integral defined by (11);

$\vartheta(\eta)$, integral defined by (19);

$\vartheta_1(\eta)$, $\vartheta_2(\eta)$, integrals defined in (21);

K_w, speed of first-order atom recombination on body surface;

K_1, parameter defining K_w/μ_w variation around a blunt body (Figs. 7 and 8);

Le, Lewis number (Pr/Sc);

m, exponent for power-law inviscid flow (16);

p, static pressure;

Pr, Prandtl number;

* Member Technical Staff, Aerophysics Department, Aerodynamics and Propulsion Research Laboratory.

$\dot{q}_w$, total heat-transfer rate per unit area;
$\dot{q}_{w_D}$, diffusion heat-transfer rate per unit area;
r, exponent for power-law inviscid flow (16);
R_B, blunt body nose radius;
r_0, local body radius (Fig. 1);
Sc, Schmidt number,
T, static temperature, absolute;
u, flow velocity in x-direction (tangent to body);
x, y, streamwise and normal body co-ordinates (Fig. 1);
z, α/α_e.

Greek symbols

α, atom mass fraction (ρ_A/ρ);
β, series solution parameter (22) and (23);
$\bar{\gamma}$, frozen specific heat ratio of mixture;
ζ, surface Damkohler number (atom-diffusion time/surface-recombination time);
η, normal similarity co-ordinate (1);
$f(\eta)$, boundary layer stream function;
λ, exponent in power-law Damkohler number distribution;
μ, viscosity coefficient;
ξ, streamwise similarity co-ordinate;
ρ, mixture mass density;
ω_n, wall gradient function (Fig. 2).

Subscripts

A, atom;
c, completely catalytic wall solution;
e, conditions at edge of boundary layer;
M, molecule;
0, reference value;
s, stagnation point conditions;
w, conditions on wall.

1. INTRODUCTION

SOLUTIONS to the diffusion equation for chemically-frozen, dissociated, laminar boundary-layer flows over catalytically-reacting surfaces have been studied extensively for constant surface temperature, catalytic efficiency, and first-order atom recombination [1–7]. These analyses entail various approximate methods of solution as well as a class of exact solutions given by Chambré and Acrivos [2]. Recently, Chung *et al.* [8] have further extended the theory to include the effects of arbitrary variations in catalytic efficiency along the surface for a fairly general class of bodies, using both the integral method and a modification of a technique developed by Lighthill [9, 10]. However, it is clearly of interest to obtain some exact analytical solutions that account for varying surface catalytic efficiency in order to appraise the accuracy of these approximate methods. Moreover, since the analyses mentioned frequently involve a good deal of numerical work in specific applications, analytical solutions are very useful in clarifying the physical behavior involved. The object of this paper is to describe both exact and approximate closed-form solutions to the boundary-layer diffusion equation in the presence of body surfaces with a first-order atom recombination rate that is distributed in any arbitrary continuous manner and to compare the results in various specific applications with those obtained by the integral, Lighthill, and local similarity methods.

Exact solutions will be developed for flat plate flow, incompressible flow over wedges, and supersonic flows around wedges or cones wherein the surface Damkohler number varies either as any power of the distance or is distributed as a polynomial in the distance. These solutions constitute a direct extension of Chambré and Acrivos by analogy with the Chapman–Rubesin treatment of heat transfer to non-isothermal surfaces [11]. To be sure, Chambré and Acrivos have pointed out the possibility of these obvious generalizations of their theory for constant catalytic efficiency and wall temperature; however, the actual analysis has not in fact been carried out and is therefore presented here. Furthermore, by imposing the assumption of local similarity in the velocity profile, it will be shown that the method may also be applied with good approximation to the case of hypersonic flow over highly-cooled bodies. Application to the particular case of blunt-body flow with varying surface catalycity around the nose will be made in detail.

The exact solutions take the form of power series in the streamwise co-ordinate along the body. In many cases of interest, it will be shown

that they satisfactorily describe a large portion of the effects due to varying catalycity along the surface. Nevertheless, the entire region of physical interest usually cannot be conveniently analysed by these methods because either a limited radius of convergence exists in certain cases or the use of a prohibitive number of series terms becomes necessary. Therefore, an approximate method is set forth for carrying the exact solutions forward throughout the entire flow field by means of a local nonlinear extrapolation of the leading term in the series solutions. This technique yields very simple closed-form relations for the atom concentration and diffusion along the surface. It is shown by several examples that the technique predicts the full exact solution (where applicable) very accurately and is also in good agreement with the predictions of other, more complicated, approximate solutions.

2. GOVERNING EQUATIONS IN THE SIMILARITY PLANE VARIABLES

A. Basic relations

Consider laminar boundary-layer flow of a dissociated binary gas mixture around a two-dimensional or axially-symmetric body (Fig. 1) with an arbitrary distribution of the atom recombination rate along the surface. The flow is taken to be chemically-frozen throughout (gas phase reactions absent) and the velocity distribution across the boundary layer is assumed locally self-similar and independent of the solutions to the energy and diffusion equations. Then, by introducing the well-known similarity co-ordinates

$$\xi(x) = C\int_0^x \rho_e\mu_e u_e r_0^{2\epsilon}\,\mathrm{d}x \qquad \left\{\begin{matrix}\epsilon = 0, \text{ two-dimensional}\\ \epsilon = 1, \text{ axisymmetric}\end{matrix}\right\} \quad (1)$$

$$\eta(x, y) = \frac{r_0^{\epsilon}u_e}{\sqrt{(2\xi)}}\int_0^y \rho\,\mathrm{d}y$$

and the assumptions

$$\rho\mu = \text{constant} = C\rho_e\mu_e \quad (2a)$$

$$C_{P_A} = C_{P_M} = \text{constant} = \bar{C}_P \quad (2b)$$

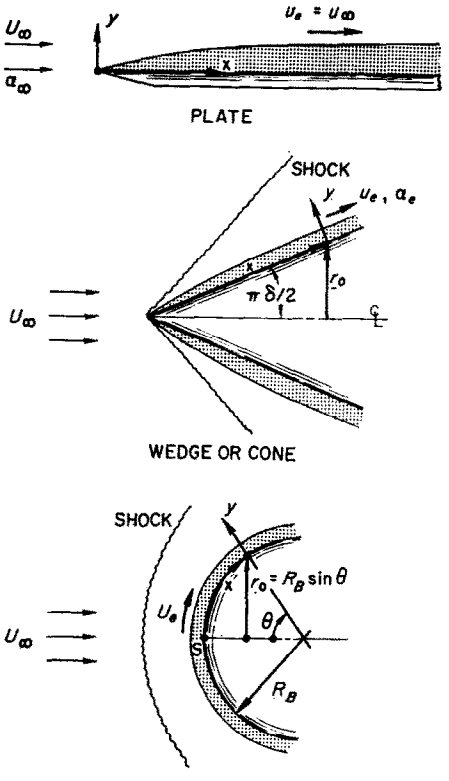

FIG. 1. Flow configuration.

the diffusion and energy equations of the boundary layer for constant Schmidt and Prandtl numbers can be written as follows:

$$Scf\frac{\partial z}{\partial\eta} + \frac{\partial^2 z}{\partial\eta^2} = 2Scf'\xi\frac{\partial z}{\partial\xi} \quad (3)$$

$$Prf\frac{\partial g}{\partial\eta} + \frac{\partial^2 g}{\partial\eta^2} = (1 - Pr)\frac{u_e^2}{2h_e}(f'^2)' + 2Prf'\xi\frac{\partial g}{\partial\xi} \quad (4)$$

where a prime ($'$) denotes differentiation with respect to η, $z = a/a_e$, $g = h/h_e$ ($h \equiv \bar{C}_P T + u^2/2$), and $f(\eta)$ is the boundary layer stream function ($f' \equiv u/u_e$). The boundary conditions on (3) and (4) are

$$f'(\infty) = z(\infty, \xi) = g(\infty, \xi) = 1 \quad (5)$$

and, at the wall

$$f(0) = f'(0) = 0, \quad g(0, \xi) = g_w(\xi) \quad (6)$$

$$\frac{\partial z}{\partial \eta}(0, \xi) = \underbrace{\left[\frac{\sqrt{(2\xi)ScK_w}}{u_e r_0^{\epsilon}\mu_w}\right]}_{\zeta(\xi)} \cdot z(0, \xi) \qquad (7)$$

where K_w is the speed of the atom recombination reaction on the surface (a function of the given surface material and temperature distribution). Equation (7) expresses the fact that the atom diffusion flux from the gas to the wall is equal to the net rate of atom recombination on the surface, here assumed to be a first-order reaction. The parameter $\zeta(\xi)$ may be interpreted as a local ratio of atom-diffusion time to surface-recombination time (Damkohler number), which determines the relative effects of surface reaction and gaseous diffusion on the atom concentration profile. When $\zeta \ll 1$, the distribution of atoms is primarily controlled by the (small) surface recombination rate in such a way that, in the limit $\zeta = 0$, the diffusion flux vanishes, leaving a uniform atom concentration $z(\eta, \xi) = 1$ across the boundary layer. On the other hand, for $\zeta \gg 1$, the atom distribution is controlled by diffusion in such a way that the surface becomes an infinite sink for atoms [$z(0, \xi) = 0$], with $\partial z/\partial \eta\ (0, \xi)$ finite in the limit $\zeta \to \infty$.

Once the diffusion and energy equations are solved, the local surface heat-transfer rate $\dot{q}_w$ may then be calculated from

$$\frac{-\sqrt{(2\xi)Pr}\dot{q}_w}{C\rho_e\mu_e u_e r_0^{\epsilon}} = h_e \frac{\partial g}{\partial \eta}(0, \xi) + Leh_D a_e \frac{\partial z}{\partial \eta}(0, \xi) \qquad (8)$$

where h_D is the dissociation energy of the gas and Le is the Lewis number (Pr/Sc).

Equations (3)–(7) constitute a two-point boundary value problem that requires the solution to a set of linear partial differential equations when $g_w(\xi)$ and $\zeta(\xi)$ are arbitrary functions of ξ. The linearity of these equations is, of course, a consequence of the assumptions concerning $\rho\mu$ and $f(\eta)$. Now, it has been shown that, when C and $\bar{C}_P$ are suitably chosen, equations (2) are good approximations for determining surface phenomena such as heat transfer, diffusion rate, and atom concentration [12, 13]. On the other hand, when $\rho\mu$ = constant, the assumption that the boundary layer velocity profile is self-similar and independent of z and g is, in fact, exact for supersonic flow over wedges and cones (f = Blasius function) or incompressible wedge flows (Falkner–Skan solutions). Moreover, with the exception of highly adverse pressure gradient regions, this assumption has proved to be a reasonably good engineering approximation for various types of bodies in hypersonic flows, including highly cooled blunt bodies [12, 14, 15].

As a result of assumption (2b) [15], the energy equation is uncoupled from the diffusion equation and the solution to each may therefore be regarded as a separate problem. Now the solution to (4) depends only on the momentum equation $f(\eta)$, the assumed distributions of wall temperature, and the inviscid flow velocity, and has been given for various cases by numerous authors [9–13, 15, 16]. Therefore, for the purpose of evaluating the effects of variable surface catalycity on the atom concentration, diffusion, and the heat transfer at the wall, our interest clearly lies in solving (3), (6), and (7) with $\zeta(\xi)$ an arbitrary function of ξ.

B. *Exact similarity solutions*

The boundary condition (7) associated with the boundary layer diffusion equation (3) does not admit a self-similar solution $z = z(\eta)$ when K_w, μ_w, μ_e, ρ_e, r_0, and u_e are arbitrary functions of ξ or x. Before treating this general case, however, let us briefly review the class of problems in which a similarity solution can be obtained. This occurs when ζ = constant = ζ_0 and the term $\partial z/\partial \xi$ in (3) may be dropped to give the ordinary differential equation

$$Scfz' + z'' = 0. \qquad (9)$$

The solution subject to the boundary conditions (6) and (7) has previously been given by Goulard [17] and is

$$z(\eta) = \frac{1 + \zeta_0 I(\eta)}{1 + \zeta_0 I(\infty)} \qquad (10a)$$

$$z'(0) = \zeta_0 z(0) = \frac{\zeta_0}{1 + \zeta_0 I(\infty)} \qquad (10b)$$

where

$$I(\eta) \equiv \int_0^\eta \exp\left(-Sc \int_0^\eta f \, d\eta\right) d\eta.^* \quad (11)$$

Hence, for a completely non-catalytic wall ($\zeta = 0$),

$$z'(0) = 0, \quad z(\eta) = 1 \quad (12)$$

whereas, in the opposite extreme of a completely catalytic wall ($\zeta_0 \to \infty$),

$$z = z_c(\eta) = \frac{I(\eta)}{I(\infty)}, \quad z_c(0) = 0,$$

$$z_c'(0) = I(\infty)^{-1}. \quad (13)$$

The solutions (10) with $0 < \zeta_0 < \infty$ pertain to all frozen boundary-layer flows for which the streamwise variations in inviscid flow properties, wall temperature, and catalytic efficiency are such that

$$\frac{K_w}{\mu_w} \sim \frac{u_e r_0^\epsilon}{\sqrt{\xi}} \quad (14)$$

that is, where the velocity of atom recombination on the surface decreases with increasing ξ at the same rate as the boundary-layer diffusion flux. Now, by equations (1) and (10b), the actual atom concentration gradient at the surface in the physical plane is

$$\frac{\partial z}{\partial y}(0, \xi) = \frac{\sqrt{(C)\rho_e \mu_e u_e r_0^\epsilon}}{\mu_w \sqrt{(2 \int_0^x \rho_e \mu_e r_0^{2\epsilon} u_e \, dx)}} z'(0) \quad (15)$$

which becomes infinite at the origin when $\zeta_0 \neq 0$ unless the wall temperature (μ_w) is appropriately distributed. To illustrate, consider the general class of flows for which $\rho_e \mu_e \sim x^a$, $\mu_w \sim x^b$, $u_e \sim x^m$, and $r_0 \sim x^r$ (a, b, m, and r being arbitrary constants). Here, self-similarity exists when the surface catalyticity is distributed as

$$K_w \sim x^{-\left(\frac{1+a-m-2b}{2}\right)} \sim \xi^{-\frac{(1+a-m-2b)}{2(1+a+m+2\epsilon r)}} \quad (16)$$

so that

$$\frac{\partial z}{\partial y}(0, \xi) \sim x^{-\left(\frac{1+2b-a-m}{2}\right)} \frac{\partial z}{\partial \eta}(0, \xi)$$

$$\sim \xi^{-\frac{(1+2b-a-m)}{2(1+a+m+2\epsilon r)}} \frac{\partial z}{\partial \eta}(0, \xi) \quad (17)$$

* When $f(\eta)$ is taken to be the Blasius function, $I(\infty) \cong (0{\cdot}47\ Sc^{1/3})^{-1}$.

will become infinite at $x \to 0$ unless $2b \leqslant -(1 - m) + a$. Physically, this condition requires that the diffusion coefficient of the gas approach infinity rapidly enough at the origin to either balance or overcome the increase in diffusion flux due to the vanishing boundary layer thickness. We note, however, that a self-similar solution having a finite $\partial z/\partial y$ (0, 0) does exist under isothermal ($b = 0$), iso-catalytic (K_w = constant) conditions in the special case of stagnation point flow ($a = 0$, $m = 1$) since the boundary layer thickness does not vanish at $x = 0$.

Although the relations (10) are exact only when ζ = constant, by invoking the idea of local similarity, they can also be made to serve as approximate solutions when the Damkohler number varies along the surface [12, 14, 15]. The local similarity concept is based on the argument that, when $\zeta(\xi)$ is sufficiently slowly-varying, one should be able to approximate the exact non-similar solution at each ξ by using (10) in conjunction with the appropriate local values of $\zeta(\xi)$. The conditions under which the flow may be considered slowly varying can be defined by an examination of the diffusion equation (3). By employing an integrating factor $\exp(Sc \int_0^\eta f \, d\eta)$, formally integrating this equation twice, and employing the boundary conditions (5) and (7), one obtains

$$z(0, \xi) = \frac{1 - 2Sc\xi \, (d/d\xi) \, [\vartheta(\infty)]}{1 + \zeta I(\infty)} \quad (18)$$

where

$$\vartheta(\eta) \equiv \int_0^\eta \exp\left(-Sc \int_0^\eta f \, d\eta\right)$$

$$\left[\int_0^\eta \exp\left(+Sc \int_0^\eta f \, d\eta\right) f'z \, d\eta\right] d\eta. \quad (19)$$

Now, by approximating $z(\eta, \xi)$ in $\vartheta(\eta)$ by the local similarity value, for the purpose of estimating the contribution of the non-similar term to (18), one obtains

$$z(0, \xi) \simeq \frac{1 + \dfrac{2Sc \, \xi \, (d/d\xi) \, I(\infty)}{1 + I(\infty)\zeta} \left[\dfrac{\vartheta_1(\infty) - \vartheta_2(\infty)}{1 + \zeta I(\infty)}\right]}{1 + \zeta I(\infty)} \quad (20)$$

where

$$\vartheta_1(\eta) \equiv \int_0^\eta \exp(-Sc\int_0^\eta f\,d\eta)\left[\int_0^\eta \exp(Sc\int_0^\eta f\,d\eta) f'\,d\eta\right] d\eta \quad (21a)$$

$$\vartheta_2(\eta) \equiv \int_0^\eta \exp(-Sc\int_0^\eta f\,d\eta)\left[\int_0^\eta \exp(Sc\int_0^\eta f\,d\eta)\frac{I(\eta)}{I(\infty)}\,d\eta\right] d\eta \quad (21b)$$

with $\vartheta_1 \geqslant \vartheta_2$ when $Sc \leqslant 1$ (11). According to (20), the local similarity approximation will be accurate when the second term in the numerator is small compared to unity. Evidently, this condition is always satisfied when $\zeta \gg 1$, that is, when the local surface is highly catalytic. However, it is not necessarily satisfied when $\zeta \lesssim 1$; hence, local similarity may not be very accurate when the surface recombination rate is small. Moreover, it is clear from (20) that local similarity will never hold in the vicinity of very abrupt changes in surface catalycity.

3. EXACT SOLUTIONS FOR ARBITRARILY-DISTRIBUTED SURFACE CATALYCITY

The diffusion equation (3) has been solved in [2] for flat plate and incompressible wedge flows when the catalytic efficiency and temperature are constant along the surface. However, it is clear by analogy with the theory of Chapman and Rubesin [11] that the solution is readily generalized to arbitrary but continuous distributions in K_w/μ_w. This extension will now be given for the important case of a first-order atom recombination rate on the surface. (More complicated, higher-order, surface recombination mechanisms could also have been treated in a similar manner if desired.) It should be noted that the present formulation is a more general one than that in [2] because it includes the Mangler and Stewartson–Illingworth transformations and is therefore applicable to supersonic flows around cones and (approximately) to hypersonic flows over slender and blunt-nosed bodies.

A. *Analysis*

As suggested in [11], a general solution to (3) is sought by separation of variables and superposition of particular solutions. Accordingly, a solution of the following form is assumed:

$$z(\eta, \xi) = 1 + \sum_{n=0} A_n \xi^{n/\beta} Z_n(\eta) \quad (22)$$

where the A_n are constants and n, β are integers with β fixed over the summation. By substituting (22) into (3), it is found that the $Z_n(\eta)$ must satisfy the ordinary differential equation

$$Scf Z_n' + Z_n'' - 2\left(\frac{n}{\beta}\right) Scf Z_n = 0. \quad (23)$$

The boundary conditions (6) and (7) require

$$Z_n(\infty) = 0 \quad (24)$$

and

$$\sum_{n=0} A_n \xi^{n/\beta} Z_n'(0) = \zeta(\xi)\left[1 + \sum_{n=0} A_n \xi^{n/\beta} Z_n(0)\right] \quad (25)$$

where it is convenient to take

$$Z_n(0) = 1 \quad (26)$$

leaving $Z_n'(0)$ to be determined. Now (25) is satisfied by all Damkohler number distributions (including the effect of variable K_w/μ_w) of the form

$$\zeta(\xi) = \sum_{\kappa=0} B_\kappa \xi^{\kappa/\beta} \ (\kappa \text{ an integer}) \quad (27)$$

when the A_n are determined from the $Z_n'(0)$ and the coefficients B_κ as follows:

$$\left.\begin{aligned} A_0 &= \frac{B_0}{Z_0'(0) - B_0} \\ A_1 &= \frac{(1 + A_0)B_1}{Z_1'(0) - B_0} \\ &\cdots \\ A_n &= \frac{(1 + A_0)B_n + \sum_{j=1}^{n-1} B_j A_{n-j}}{Z_n'(0) - B_0} \end{aligned}\right\} \quad (28)$$

Thus, (22) is an exact solution to (3) whenever ζ is a Taylor or fractional power series in ξ. The atom concentration at the wall and the gradient normal to the surface are given by

$$z(0, \xi) = \frac{Z_0'(0)}{Z_0'(0) - B_0} + \sum_{n=1} A_n \xi^{n/\beta} \quad (29)$$

$$\frac{\partial z}{\partial y}(0, \xi) = \frac{C\rho_e\mu_e u_e r_0^\epsilon}{\mu_w\sqrt{(2\xi)}} \times \left[\frac{B_0 Z_0'(0)}{Z_0'(0) - B_0} + \sum_{n=1} A_n Z_n'(0)\xi^{n/\beta}\right]. \quad (30)$$

The local heat transfer due to diffusion is then given by $\dot{q}_{w_D} = (\mu_w h_D a_e/Sc)\partial z/\partial y(0, \xi)$. Since $Z_0'(0) = -[I(\infty)]^{-1}$, (10b) shows that the leading terms in (29) and (30) are the similarity solutions pertaining to a uniform surface catalycity $\zeta = \zeta_0 = B_0$. Therefore, (30) yields an infinite diffusion heat transfer at $\xi = 0$, unless: (a) μ_w times the coefficient of the bracketed term is a constant or vanishes at $\xi = 0$ when $B_0 \neq 0$, or (b) the surface at the origin is completely non-catalytic ($B_0 = 0$) and the rate at which ζ approaches zero at the origin is sufficiently large to balance or overcome the corresponding effect of the vanishing boundary layer thickness. As an example, for the class of inviscid flows and body shapes defined above in connection with (16), condition (a) gives $0 \leqslant -(1 - m) + a$, while condition (b) requires that

$$0 < \beta < \frac{2(a + m + 1 + 2\epsilon r)}{1 - a - m}, \quad m \neq 1.$$

When ζ varies as a single power of the distance, that is,

$$\zeta = B_\lambda \xi^\lambda \tag{31}$$

where B_λ is a constant and λ is any non-zero positive or negative number, two special cases of the foregoing general solution can be found by writing $\partial z/\partial \xi = (\partial z/\partial \zeta)\,(\mathrm{d}\zeta/\mathrm{d}\xi)$ in (3), assuming series solutions in ascending positive or negative powers of ζ, and then proceeding in the same manner as described above. The resulting solutions are

$$\left.\begin{aligned} z(\eta, \xi) &= 1 + \sum_{n=1} A_n' \zeta^n Z_n(\eta) \\ &= 1 + \sum_{n=1} A_n \xi^{n\lambda} Z_n(\eta) \\ A_n = (B_\lambda)^n A_n' &= \frac{B_\lambda^n}{\prod_{j=0}^{n} Z_j'(0)}, \quad (\lambda > 0) \end{aligned}\right\} \tag{32}$$

and

$$\left.\begin{aligned} z(\eta, \xi) &= z_c(\eta) + \sum_{n=1} A_n' \zeta^{-n} Z_n(\eta) \\ &= z_c(\eta) + \sum_{n=1} A_n \xi^{|n\lambda|} Z(\eta) \\ A_n = \frac{A_n'}{B_\lambda^n} &= -\frac{\prod_{j=0}^{n=1} Z_j'(0)}{B_\lambda^n}, \quad (\lambda < 0) \end{aligned}\right\} \tag{33}$$

where $Z_n(\eta)$ and $Z_n'(0)$ are obtained from (33) by replacing β^{-1} with $|\lambda|$. The solutions (32) for $\lambda > 0$ involve an increasing surface catalycity along the body and were previously obtained by Chambré and Acrivos for constant K_w/μ_w on either isothermal flat plates ($\lambda = 1/2$) or wedges in incompressible flow

$$[\lambda = (1 - m)/2(1 + m) = (1 - \delta)/2,$$

where $\pi\delta$ is the wedge apex angle and $u_e \sim x^m$]. However, the present theory further includes the general class of flows cited in connection with (16), as well as any variation of catalytic efficiency and temperature along the surface for which $K_w/\mu_w \sim x^d$ (d = arbitrary constant), by merely adjusting λ according to

$$\lambda = \frac{1 + a + 2d - m}{2(1 + a + m + 2\epsilon r)} \tag{34}$$

provided $d > -[(1 + a + m)/2]$, ($\lambda > 0$). For such flows, (17) and (32) indicate that there is no singularity in diffusion heat transfer at the origin, provided

$$\lambda \geqslant \frac{1 - a - m}{2(1 + a + m + 2\epsilon r)}, \text{ (i.e. } d \geqslant -a). \tag{34}$$

The solutions (33) for $\lambda < 0$ are apparently new and represent flow along a surface whose catalycity is decreasing with distance. It can be seen from (17) and (33) that these solutions yield an infinite diffusion heat transfer at the origin regardless of the value of λ unless

$$0 \leqslant -(1 - m) + a.$$

The boundary value problem (23, 24, 26) possesses unique solutions for all values of $n/\beta \geqslant -1/2$, and these have been studied extensively by various investigators for both plate and incompressible wedge flow boundary-layer velocity distributions [11, 18]. Therefore, $Z_n(\eta)$ and $Z_n'(0)$ may be regarded as known functions in the present analysis. A plot of $Z_n'(0)$ versus n/β and Sc based on the Blasius profile is given in Fig. 2 to illustrate the typical behavior of the gradient function. It may be seen from Fig. 2 and Cauchy's ratio test [19] that the series solution (32) for the special class of flows (31) is absolutely convergent for all $\zeta(\xi)$, although the convergence becomes slow when $\zeta \geqslant 1$. On

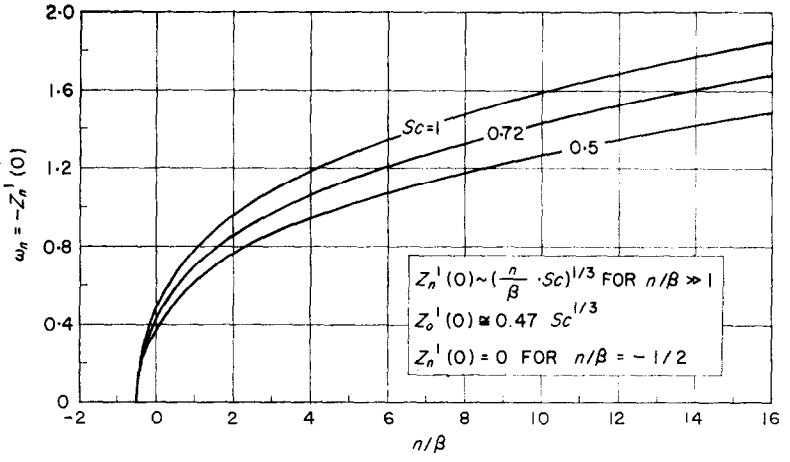

FIG. 2. Wall gradient function $Z_n'(0)$.

the other hand, by the same criterion, the series (33) for $\lambda < 0$ is found to be divergent for all ζ; however, a more detailed study shows that this series is, in fact, of a semi-convergent character. In view of this property, and since (22) and (32) cover most of the problems of practical interest, these solutions for $\lambda < 0$ will not be considered further in this paper.

In the case of polynomial Damkohler number distributions, the comparison test shows that the series solution (22) will converge over a given region whenever (27) is also convergent in this region and $A_n \leqslant B_n$, although this condition becomes unnecessarily restrictive when (27) involves only a finite number of terms. However, one cannot formulate any general criterion for this convergence requirement, since the A_n depend not only on B_n but also on all the B_{n-1} and A_{n-1} as well; each specific type of distribution must be evaluated individually. It will be shown below that the solutions for this class of distributions in catalycity are of practical interest.

B. *Example application: flat plate flow*

Steady laminar boundary-layer flow on a flat plate or a wedge in supersonic flow

$$(m = a = \epsilon = 0,\ \xi = C\rho_e\mu_e u_e x)$$

is a particularly convenient and yet representative physical model with which to illustrate the salient features of the foregoing exact solutions for various types of Damkohler number distributions. In particular, it is of interest to examine variations in surface catalycity along the plate of the type (31) by assuming

$$\frac{K_w}{\mu_w} = \frac{K_{w_0}}{\mu_{w_0}} x^d, \qquad \left(\frac{K_{w_0}}{\mu_{w_0}} = \text{a constant}\right)$$

so that $\lambda = (1/2) + d$ and

$$B_\lambda = \frac{\sqrt{(2)\ Sc\ K_{w_0}}}{\mu_{w_0} u_e\ (C\rho_e\mu_e u_e)^d}.$$

Here, it is convenient to switch from ξ to x by writing $\zeta = B_\lambda \xi^\lambda = B_\lambda' x^\lambda$ where

$$B_\lambda' = \frac{Sc\ K_{w_0}}{u_e \mu_{w_0}} \sqrt{(2C\rho_e\mu_e u_e)}$$

and $\lambda = (1/2) + d$. Typical distributions of the atom concentration and diffusion heat transfer along the plate surface, as given by the first ten and fifteen terms of the series (31), are shown in Figs. 3 and 4, respectively, for $Sc = 0{\cdot}72$ and $\lambda = 1/2$ [2], 1, 3/2, and 2.* The abscissae and the ordinates of the diffusion curves used in these figures were chosen because they render the solutions in a universal form applicable to any combination of the inviscid flow and gas properties. It is seen that the first ten series terms are sufficient to accurately describe more than 50 per cent of the maximum

* Using a desk calculator, each of these cases required less than an hour to compute for the range of x and ζ shown in Figs. 3 and 4.

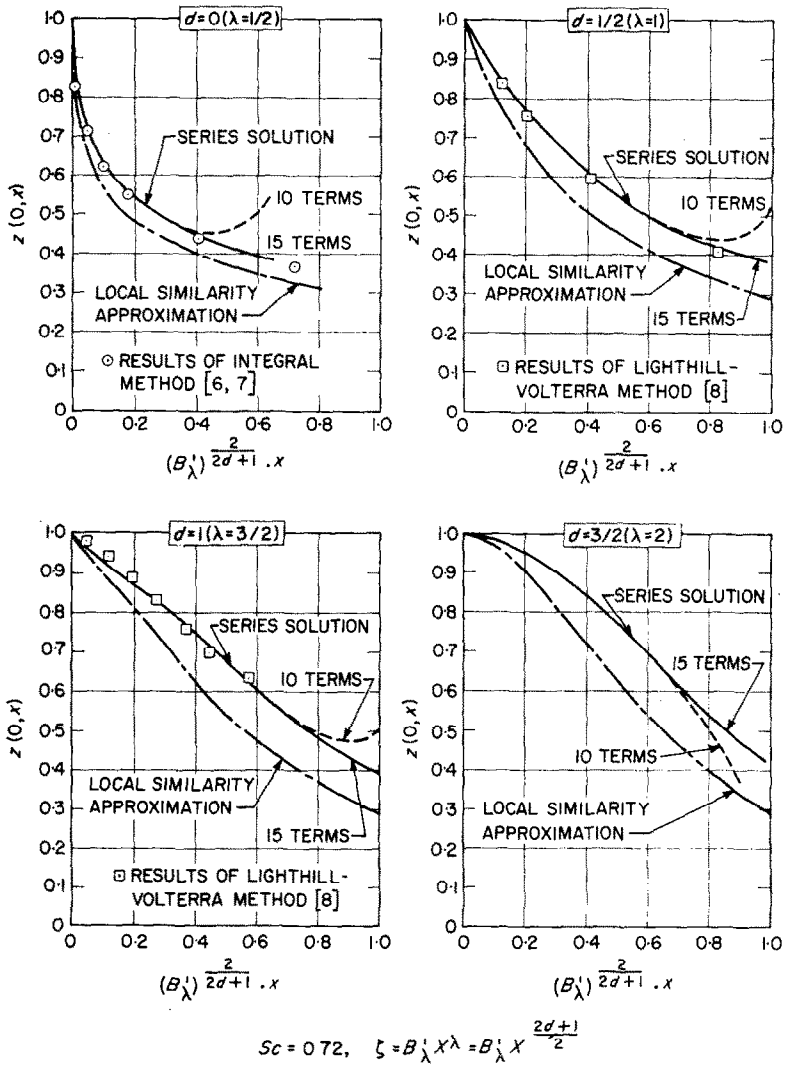

FIG. 3. Variation of atom concentration along a plate for power law distributions of the surface catalycity.

total decrease in atom concentration and 75 per cent of the corresponding increase in heat transfer (the variation in the former appreciably lagging behind the latter) that can occur downstream of the non-catalytic leading edge because of the increase in Damkohler number with x. To be sure, the slow convergence of the series for $\zeta > 1$ generally limits the usefulness of the solution in terms of x to a relatively small region near the leading edge. Nevertheless, when judged on the basis of the streamwise variations in surface phenomena that can be analysed, these exact series solutions provide an easily calculated and relatively simple description of a significant portion of the flow field for surface reaction distributions of the type (31). There are also shown in Figs. 3 and 4 the local similarity solutions appropriate to each λ, the approximate surface atom concentration distributions obtained by Chung *et al.* [8] for $\lambda = 1$ and 3/2 using a modified Lighthill method, and the result for $\lambda = 1/2$ obtained by Chung and Anderson [6] by an integral method. In view of (20) and the rapid variations taking place downstream of the

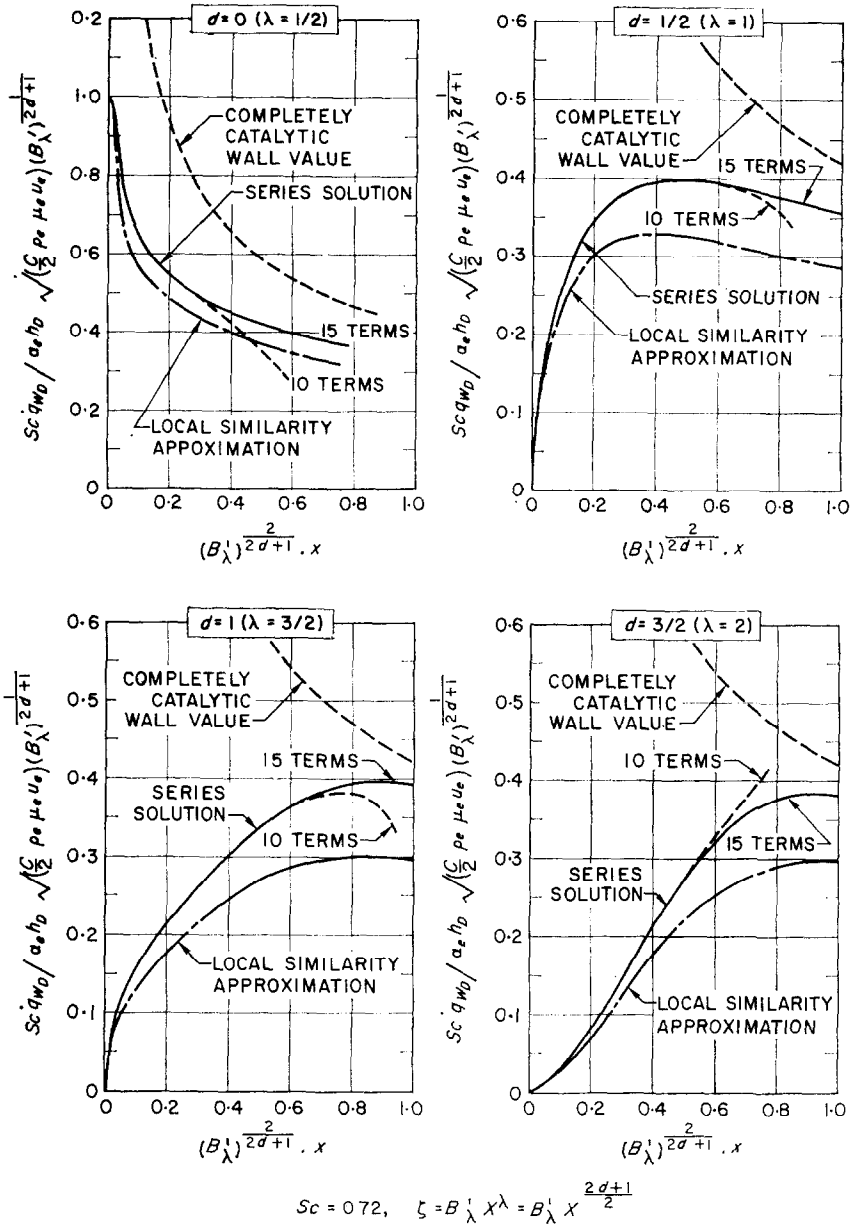

FIG. 4. Variation of diffusion heat transfer along a plate for power law distributions of the surface catalycity.

leading edge, local similarity yields an understandably poor quantitative approximation to both $z(0, x)$ and $\partial z/\partial y$ $(0, x)$ in these examples (except for extremely small x), the inaccuracy increasing with λ. As predicted by (20), the nonsimilar effect causes the value of $z(0, x)$ to lie above the corresponding local similarity solution. Note, however, that the exact solutions do tend to become parallel to the local similarity curves. On the other hand, the results of [6] and [8] are seen to be in good agreement with the present solutions, which supports the generally accepted

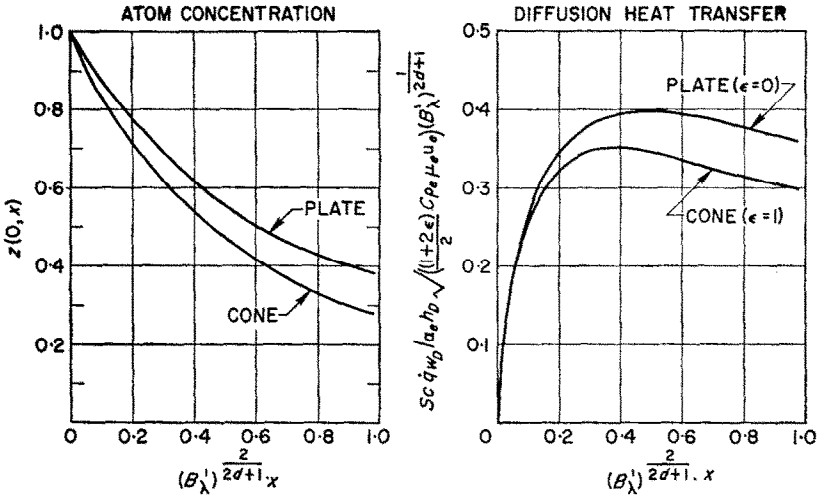

FIG. 5. Comparison of exact solutions for a flat plate and cone.

confidence in the accuracy of the Lighthill and integral methods.*

It may be seen that the solutions for a cone in supersonic flow [$\epsilon = r = 1, m = a = 0$, $\xi = C\rho_e\mu_e u_e (\sin^2\delta/2)(x^3/3)$] differ in only two respects: a value of $\lambda = (1/3)\lambda_{\text{plate}} = 1/6 + d/3$ is used in obtaining the $Z_n'(0)$ in (32), and $B_\lambda' = (B_\lambda')_{\text{plate}}/\sqrt{3}$. Consequently, the distributions of $z(0, x)$ and $\dot{q}_{w_D}$ along the cone surface for a given value of d, when plotted in the manner of Figs. 3 and 4, will be quite similar to the results for a flat plate. This is illustrated in Fig. 5 for the case $d = 1$, where solutions for both a plate and cone are presented.

C. *Hypersonic flow around a blunt body*

By assuming a locally self-similar boundary-layer velocity profile, equations (19) and (29) may also be used to described (approximately) the effects of finite surface catalycity on frozen boundary-layer flows over bodies other than plates, wedges, or cones. An important example of such an application is the stagnation-region flow around a blunt body in a hypersonic stream. Here, an exact similarity solution to the diffusion equation does not exist downstream of the stagnation point because of the strong inviscid pressure gradient associated with the rapid expansion around the nose. We shall now show that the present solution for a polynomially distributed Damkohler number is capable of describing satisfactorily this non-linear behavior.

Consider the stagnation region of a hemisphere or cylinder (Fig. 1) and regard the inviscid flow as frozen in dissociation by the expansion around the body [$\alpha_e(x) = \alpha_s$]. Here $r_0 = R_B \sin\theta$ and the local pressure can be represented by a Newtonian distribution

$$\frac{p_e(x)}{p_s} = \cos^2\theta \simeq 1 - \theta^2 + \frac{3}{4}\theta^4 - \frac{7}{12}\theta^6 + \ldots . \tag{35}$$

This series representation gives a good approximation up to $\theta \lesssim 60°$; more terms could, of course, be included to go further around the nose if desired. From the isentropic relation

$$\frac{p_e}{p_s} = \left(\frac{\rho_e}{\rho_s}\right)^{\bar{\gamma}_e}$$

and the inviscid momentum equation, the corresponding local velocity is

$$\frac{u_e}{B_s x} = 1 - \left(\frac{3\bar{\gamma}_e - 2}{8\bar{\gamma}_e}\right)\theta^2 + \left(\frac{85\bar{\gamma}_e^2 - 44\bar{\gamma}_e + 20}{4 \times 96\bar{\gamma}_e^2}\right)\theta^4 - \ldots \tag{36}$$

* These results were kindly provided by P. M. Chung and S. W. Liu in a private communication.

where

$$B_s = \left(\frac{du_e}{dx}\right)_s = \sqrt{\left(\frac{2p_s}{\rho_s}\right)} R_B^{-1}$$

and $\bar{\gamma}_e$ is the frozen specific heat ratio for the inviscid flow. For the purpose of illustrating the essential features of the solution, we postulate a linear viscosity–temperature relationship for the inviscid flow and consider variations in K_w/μ_w long the body of the form

$$\frac{K_w}{\mu_w} = \frac{K_{w_s}}{\mu_{w_s}}(1 + K_1\theta^d)$$

(where K_1 and $d > 0$ are arbitrary). Then, from (1) and (7), respectively, are obtained

$$\xi' \equiv \frac{2(1+\epsilon)\xi}{\rho_s\mu_s B_s R_B^{2(1+\epsilon)}} = \theta^{2(1+\epsilon)} \times \left[1 - \left(\frac{\epsilon+1}{\epsilon+2}\right)\underbrace{\left(\frac{11\bar{\gamma}_e - 2}{8\bar{\gamma}_e} + \frac{2\epsilon}{3}\right)}_{a_2}\theta^2 + \left(\frac{1+\epsilon}{3+\epsilon}\right)a_4\theta^2 - \left(\frac{1+\epsilon}{4+\epsilon}\right)a_6\theta^6 + \ldots\right] \quad (37)$$

$$\zeta(\theta) = \zeta_s(1 + K_1\theta^d) \times \left[1 - \underbrace{\left(\frac{a_2}{2} - \frac{3\bar{\gamma}_e - 2}{8\bar{\gamma}_e} - \frac{\epsilon}{3}\right)}_{b_2}\frac{\theta^2}{2} + b_4\frac{\theta^2}{2} - b_6\frac{\theta^6}{2} + \ldots\right] \quad (38)$$

where a_2, a_4, a_6, b_2, b_4, and b_6 are given as functions of $\bar{\gamma}_e$ and ϵ in Table 1, and where

$$\zeta_s \equiv \sqrt{\left[\frac{C\rho_s\mu_s}{(1+\epsilon)B_s}\right]} Sc\frac{K_{w_0}}{\mu_{w_0}}. \quad (39)$$

The variation of this parameter with flight conditions and surface catalycity is illustrated in Fig. 6. Equation (38) is valid as long as $\zeta \geqslant 0$. Now, (37) may be inverted to obtain $\theta = \theta(\xi')$ [19], and the Damkohler number distribution thereby expressed as a function of ξ'; accordingly, there results

$$\theta(\xi) = (\xi')^{1/2(1+\epsilon)}\left[1 + c_2(\xi')^{1/(1+\epsilon)} - c_4(\xi')^{2/(1+\epsilon)} + \ldots\right] \quad (40)$$

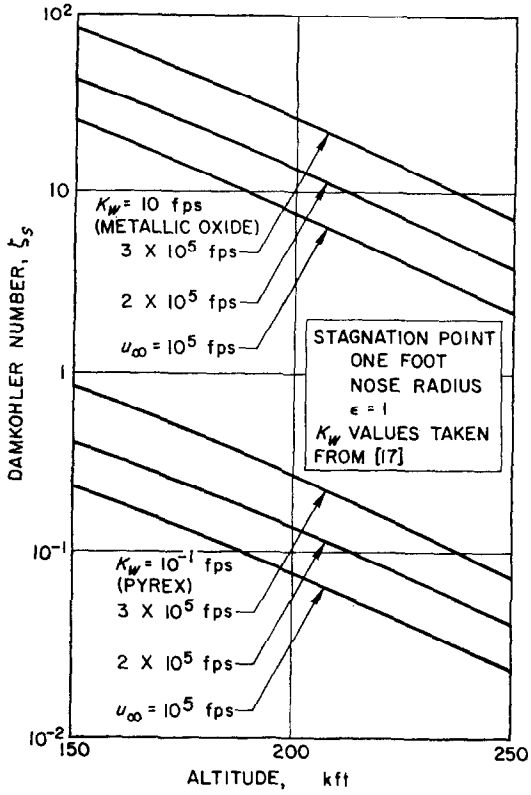

FIG. 6. Variation of surface reaction parameter with flight condition.

and

$$\frac{\zeta(\xi')}{\zeta_s} = 1 - \frac{b_2}{2}(\xi')^{1/(1+\epsilon)} + (b_4 - 2c_2b_2)(\xi')^{2/(1+\epsilon)} - \ldots + K_1(\xi')^{d/2(1+\epsilon)} \times \Big(1 - (b_2 - dc_2)(\xi')^{1/(1+\epsilon)} + \Big\{b_4 - 2c_2b_2 - d\left[c_4 + c_2b_2 - \left(\frac{d-1}{2}\right)c_2^2\right]\Big\}(\xi')^{2/(1+\epsilon)} - \ldots\Big). \quad (41)$$

The values of c_2 and c_4 are also shown in Table 1. It may be noted from this table that the coefficients in (40) and (41) depend rather weakly on $\bar{\gamma}_e$ and, therefore, on α_s.

Since the polynomial (41) reduces to the form

Table 1. Blunt body flow coefficients

Coefficient	$\bar{\gamma}_e = 1{\cdot}1$		$\bar{\gamma}_e = 1{\cdot}25$		$\bar{\gamma}_e = 1{\cdot}40$		$\bar{\gamma}_e = 1{\cdot}55$		$\bar{\gamma}_e = 1{\cdot}67$	
	$\epsilon = 0$	$\epsilon = 1$	$\epsilon = 0$	$\epsilon = 1$	$\epsilon = 0$	$\epsilon = 1$	$\epsilon = 0$	$\epsilon = 1$	$\epsilon = 0$	$\epsilon = 1$
a_2	1·148	1·815	1·175	1·842	1·196	1·863	1·214	1·881	1·225	1·892
a_4	0·982	2·646	1·021	2·703	1·053	2·749	1·079	2·787	1·102	2·817
a_6	0·766	2·948	0·794	3·022	0·816	3·081	0·834	3·129	0·846	3·165
b_2	0·278	0·247	0·238	0·211	0·205	0·183	0·179	0·160	0·162	0·144
b_4	0·035	0·217	0·020	−0·229	0·0081	−0·239	−0·0014	−0·247	−0·011	−0·255
b_6	−0·061	−0·563	−0·048	−0·575	−0·036	−0·602	−0·024	−0·590	−0·0097	−0·591
c_2	0·287	0·302	0·294	0·307	0·299	0·311	0·303	0·313	0·306	0·315
c_4	0·098	0·166	0·101	0·168	0·104	0·170	0·106	0·172	0·109	0·173

(27) for any value of $d > 0$, it is clear that solutions (28) through (30) may be applied to blunt body flows. As an example, let us consider the case $d = 1$, for which

$$\frac{\zeta(\xi')}{\zeta_s} = 1 + K_1(\xi')^{1/\beta} - b_2(\xi')^{2/\beta} - K_1(b_2 - c_2)(\xi')^{3/\beta} + (b_4 - 2c_2b_2)(\xi')^{4/\beta} + \ldots \quad (42)$$

with $\beta = 2(1 + \epsilon)$. When $f(\eta)$ is approximated by the Blasius function in the case of highly cooled walls [12], the leading terms in the series solutions for $z(0, \xi')$ and $\dot{q}_{w_D}$ are

$$z(0, \xi') = \frac{0{\cdot}47Sc^{1/3}}{0{\cdot}47Sc^{1/3} + \zeta_s}\left\{1 - \left(\frac{\zeta_s}{\omega_1 + \zeta_s}\right)K_1(\xi')^{1/\beta} - \left[\frac{b_2(\omega_1 + \zeta_s) + K_1^2\zeta_s}{\omega_2 + \zeta_s}\right](\xi')^{2/\beta} + \ldots\right\} \quad (43a)$$

$$= z(0, 0)\left\{1 - \left(\frac{\zeta_s}{\omega_1 + \zeta_s}\right)K_1\theta - \left[\frac{b_2(\omega_1 + \zeta_s) + K_1^2\zeta_s}{\omega_2 + \zeta_s}\right]\theta^2 + \ldots\right\} \quad (43b)$$

and

$$\dot{q}_{w_D}(\xi') = h_D a_s Sc^{-1}\zeta_s z(0, 0)\sqrt{[C\rho_s\mu_s B_s(1 + \epsilon)]} \times \left[1 + \frac{\omega_1 K_1}{\omega_1 + \zeta_s}(\xi')^{1/\beta} - \left\{\frac{[b_2(\omega_1 + \zeta_s) + K_1^2\zeta_s]\omega_2}{(\omega_1 + \zeta_s)(\omega_2 + \zeta_s)} + \frac{(3 + \epsilon)a_2}{2(1 + \epsilon)}\right\}(\xi')^{2/\beta} + \ldots\right] \quad (44a)$$

$$= \dot{q}_{w_D}(0)\left[1 + \left(\frac{\omega_1 K_1}{\omega_1 + \zeta_s}\right)\theta - \left\{\left[\frac{b_2(\omega_1 + \zeta_s) + K_1^2\zeta_s}{(\omega_1 + \zeta_s)(\omega_2 + \zeta_s)}\right]\omega_2 + \frac{(3 + \epsilon)a_2}{2(1 + \epsilon)}\right\}\theta^2 + \ldots\right] \quad (44b)$$

where $\omega_n \equiv -Z_n'(0)$. Here, the zero'th-order terms correspond to the self-similar stagnation point solution given by Goulard [17]. The complete solutions for the surface atom concentration and diffusion heat-transfer distributions around a hemisphere, using series terms up to and including θ^6, are shown in Figs. 7 and 8, respectively, for $Sc = 0{\cdot}72$, $\alpha_s = 0{\cdot}5$ ($\bar{\gamma}_e = 1{\cdot}53$), and various degrees of stagnation point catalycity. For each ζ_s, solutions are shown for constant wall temperature and catalycity ($K_1 = 0$) and also for both increasing and decreasing K_w/μ_w around the nose. For $\xi' < 1$ ($\theta \leqslant 57{\cdot}3°$), these solutions converge very rapidly and were easily computed on a desk calculator.

It is seen that, when $K_1 \leqslant 0$, the expansion around the nose decreases the local surface catalycity relative to the stagnation point for all $0 \leqslant \zeta_s \leqslant \infty$. This is because the Damkohler number decreases monatonically with θ as a combined result of the reduction in the boundary-layer diffusion time associated with the dropping pressure and rising velocity, and the increasing surface recombination time when $K_1 < 0$ (38). When $K_1 \leqslant -1$, the latter effect can substantially accelerate the approach toward

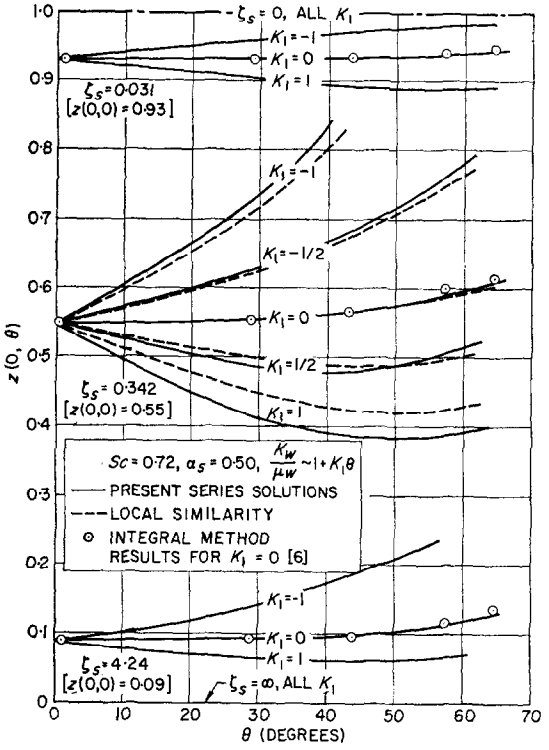

FIG. 7. Surface atom concentration distribution on the surface of a hemisphere.

non-catalytic behavior downstream of the stagnation point even when ζ_s is large. On the other hand, the atom concentration and diffusion flux do not increase and decrease, respectively, in a monatonic manner around the nose when K_w/μ_w increases linearly with θ. Here, the increasing surface recombination rate competes with the effect of the inviscid expansion and initially increases the effective surface catalycity as the flow proceeds around the nose. At a certain value of θ, which increases rapidly with K_1, $z(0, \theta)$ and $\dot{q}_{w_D}(\theta)$ reach a minimum and maximum, respectively. This happens when the effect of the expansion eventually becomes large enough to balance out (and subsequently override) the effect of increasing K_w/μ_w. It is clear that if K_w/μ_w is distributed quadratically in $\theta (d = 2)$, a certain value of $K_1 > 0$ would exist such that either the atom concentration or heat transfer would remain constant throughout most of the nose region. When $d \geqslant 3$ and $K_1 > 0$, it is likewise clear that maxima and minima in $z(0, \theta)$ and $\dot{q}_{w_D}(\theta)$, respectively, would appear downstream of the stagnation point. Here, the surface would at first become effectively less catalytic with increasing θ and then, beyond a certain distance, pass over to an increasingly catalytic behavior as the effect of K_w/μ_w attains predominance over the influence of the expansion.

Unless $|K_1|$ is large ($\gtrsim 1$), Figs. 7 and 8 show the surface atom concentration and catalycity to be slowly varying with θ up to $\theta \approx 60°$ for all values of ζ_s. Consequently, the local similarity approximations indicated in these figures are in understandably good agreement with the series solutions. (Of course, when K_1 is not small and/or more rapid variations of K_w/μ_w with θ are considered, the local similarity theory will be far less satisfactory.) It may be noted that the variation of $z(0, \theta)$ with θ for any K_1 becomes less pronounced when the stagnation point catalycity approaches either of its two extreme values. Indeed, an examination of the leading terms in the series solution (43b) shows that $z(0, \theta) \to 1$

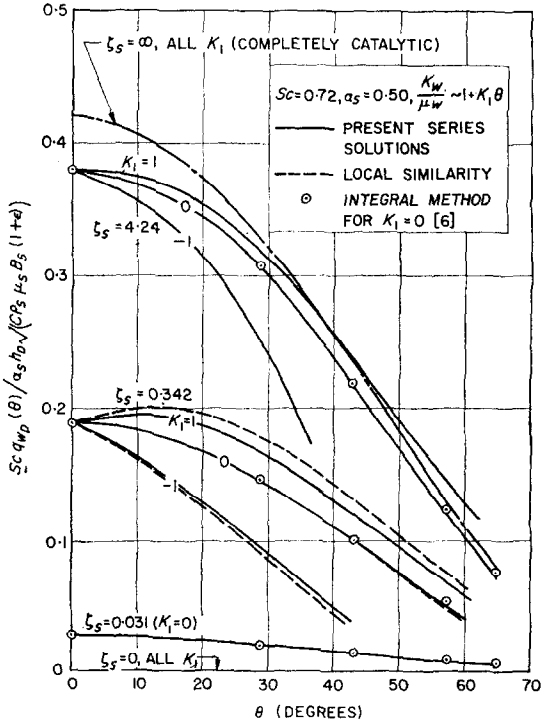

FIG. 8. Diffusion heat-transfer distribution around a hemisphere.

when $\zeta_s \to 0$ and $z(0, \theta) \to 0$ when $\zeta_s \to \infty$ for any finite K_1.* It may, in fact, easily be verified that this limiting behavior is true for all types of K_w/μ_w distributions in addition to the linear variation illustrated here.

The results of Chung and Anderson for the $K_1 = 0$ case, obtained by means of a von Kármán–Pohlhausen integral method, are shown in Figs. 7 and 8 and are seen to be in excellent agreement with the present series solutions.

4. EXTENSION OF THE SERIES SOLUTION TO THE ENTIRE FLOW FIELD

Although the foregoing series solutions satisfactorily describe a significant portion of the change in surface properties due to varying surface catalycity, they are usually unsatisfactory for treating the entire streamwise extent of the flow field in many problems of interest because of the prohibitive number of slowly converging series terms that must be used. Consequently, it would be very useful to have a simple approximate method of carrying these solutions forward throughout the entire flow field.

Recently, Rae [20] has studied theoretically the effects of homogeneous non-equilibrium dissociation near the leading edge of a flat plate by a series solution involving ascending powers of the homogeneous reaction Damkohler number. As a result of this analysis, Rae devised a relatively simple but accurate empirical method of extending his first-order solutions to a region downstream of the leading edge that is far beyond the actual radius of convergence of the first-order terms. In view of this success and the qualitative similarity between the methods of solution employed here and in [20], one is therefore naturally led to the idea of adapting Rae's approach to problems involving heterogeneous surface reactions.

To bring out the essential arguments involved, consider frozen dissociated boundary-layer flows over a flat plate, wedges, or cones in the case where the surface catalycity varies according to the simple power law (31) with $\lambda \geqslant 0$.

* When $\zeta_s \to 0$, (44b) shows that $\dot{q}_{w_D}(\theta)$ also approaches zero everywhere. On the other hand, when $\zeta_s \to \infty$, $\dot{q}_{w_D}(0)$ is a constant and $\dot{q}_{w_D}(\theta)$ decreases with θ because of the increasing boundary-layer thickness as the flow expands around the nose.

According to (32), the leading first-order terms in the full series solutions for the change in atom concentration and diffusion along the surface are

$$z(0, \xi) = 1 - \frac{\zeta(\xi)}{\omega_1} + \ldots \tag{45}$$

$$\frac{\partial z}{\partial \eta}(0, \xi) = \frac{\sqrt{(2\xi)}\,\mu_w\,(\partial z/\partial y)\,(0, \xi)}{C\rho_e\mu_e u_e r_0^{\varepsilon}} = \zeta(\xi) - \ldots \simeq \omega_1[1 - z(0, \xi)] \tag{46}$$

where $\omega_1\,(Sc, \lambda) = -Z_n'(0)$ is obtained from Fig. 2 for any chosen value of

$$\beta^{-1} = \lambda \equiv \frac{\xi}{\zeta}\frac{\mathrm{d}\zeta}{\mathrm{d}\xi}.$$

By differentiating (46) with respect to ξ, it may also be noted that, to first-order, λ is related to the streamwise variation of the surface diffusion as

$$\lambda \simeq \frac{\xi\,(\mathrm{d}/\mathrm{d}\xi)\,[(\partial z/\partial \eta)\,(0, \xi)]}{(\partial z/\partial \eta)\,(0, \xi)} \equiv \lambda'. \tag{47}$$

Equations (45), (46) and (47) are of course valid only for $\zeta \ll 1$. However, following Rae, we now seek to extrapolate these first-order solutions to arbitrary values of ζ by making the following assumption: the relationship (46) between $z(0, \xi)$ and $\partial z/\partial \eta\,(0, \xi)$, which is rigorous only for $\zeta \ll 1$, is in fact the correct form of the solution along the surface at all ζ, provided that $\omega_1(\lambda)$ is based on the value $\lambda \simeq \lambda'$ given by (47). Substituting the boundary condition (7) into (46), one thus obtains the following local approximation:

$$z(0, \xi) \approx \frac{\omega_1(\lambda')}{\omega_1(\lambda') + \zeta} = \frac{(\partial z/\partial \eta)\,(0, \xi)}{\zeta}. \tag{48}$$

The corresponding value of λ' is found by differentiating (48) with respect to ξ, holding ω_1 constant:

$$\lambda' \cong z(0, \xi)\left(\xi\,\frac{\mathrm{d}\zeta/\mathrm{d}\xi}{\zeta}\right) = z(0, \xi)\lambda. \tag{49}$$

At $\zeta \to 0[z(0, \xi) \to 1]$, these relations become exact since $\lambda' \to \lambda$; therefore, they give the correct initial values and streamwise gradients in the surface atom concentration and diffusion flux. On the other hand, at large ζ, where the wall

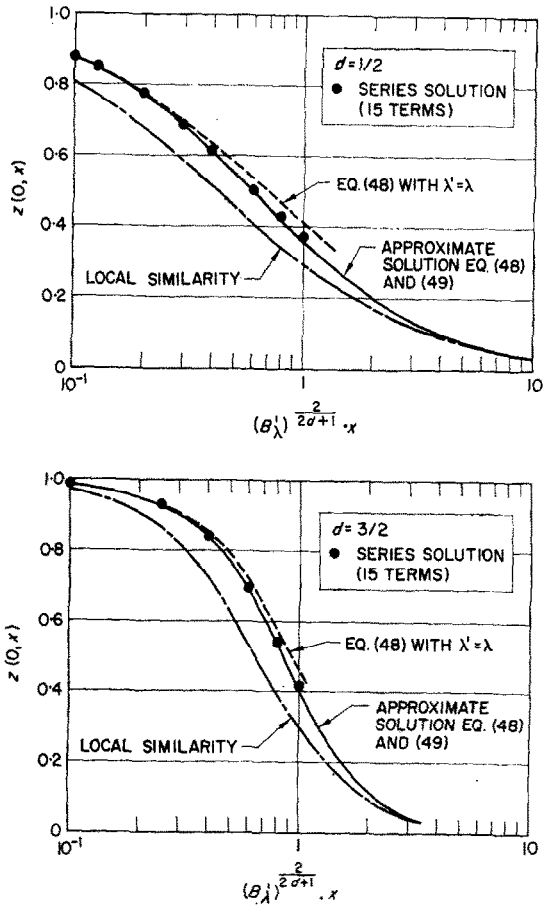

FIG. 9. Comparison of exact and approximate solutions.

approaches a completely catalytic condition [$z(0, \xi) \to 0$], (48) and (49) predict the correct asymptotic behavior since

$$\omega_1(\lambda') \to \omega_0 = 0{\cdot}47Sc^{1/3} \text{ when } \lambda' \to 0.$$

The foregoing approximation enables a very simple and rapid calculation of the atom concentration and diffusion flux distributions along the surface. By specifying the concentration [obtaining λ' and ω_1 for a given λ from (49) and Fig. 2, respectively], the streamwise station $\zeta(x)$ corresponding to it may then be found from (48). To evaluate the accuracy of the method, application has been made to several cases of flat plate flow previously treated by the full series solution; a comparison of the two theories, shown in Fig. 9, indicates an excellent agreement. Indeed, it is seen that the first approximation based on $\lambda' = \lambda$ gives a close representation of the first ten terms of the series solution for $\zeta \leqslant 1$. The approximate local theory also gives the proper behavior when $\zeta \gg 1$, correctly merging into the local similarity solution when ζ becomes slowly varying at large x. From these results, it may be concluded that the proposed approximate method of extrapolating the first-order solution to arbitrary values of x will provide an accurate description of the composition field around plates, cones, and wedges when the surface catalycity is distributed according to the power law (31).

5. CONCLUDING REMARKS

In this paper, we have studied some new solutions to the diffusion equation for frozen, dissociated, laminar boundary-layer flows over bodies with an arbitrary continuous distribution of first-order atom recombination rate along the surface. The analysis extends the theory of Chambré and Acrivos to plate, wedge, and cone flows along which the surface Damkohler number varies as any power or polynomial function of the streamwise distance. It was shown that these exact solutions, which take the form of power series that are easily evaluated on a desk calculator, satisfactorily describe a significant portion of the variations in atom concentration and diffusion heat transfer due to variable surface catalycity. Moreover, by imposing the assumption of local similarity in the velocity profile, these series solutions were shown to be good approximations for hypersonic flows around highly cooled blunt bodies with varying surface catalycity around the nose.

An approximate solution, based on an empirical method devised by Rae [20] for gas phase reactions, was also given. It provides an extremely simple closed form representation of the exact series solutions throughout the entire flow field by means of a local nonlinear extrapolation of the leading series terms. It was shown by several examples that this method yields very accurate results for the distribution of atom concentration and heat transfer along the surface for a variety of streamwise variations in wall catalycity.

Although the present analysis considers only

first-order atom recombination, it may be readily extended to higher-order surface reactions by appropriately generalizing the treatment of Chambré and Acrivos. Moreover, it may be noted that the approximate technique of a local nonlinear extrapolation of first-order series solutions developed here for continuously distributed surface reactions is also applicable to flows which discontinuously varying surface catalycity [8].

ACKNOWLEDGEMENT

The author would like to express his appreciation to Miss Dawn Martin for her assistance in obtaining the numerical solutions presented herein.

REFERENCES

1. S. M. SCALA, Hypersonic stagnation heat transfer to surface having finite catalytic efficiency, *Proc. U.S. Nat. Congr. Appl. Mech.*, 799–806 (1958).
2. P. L. CHAMBRÉ and A. ACRIVOS, On chemical surface reactions in laminar boundary layer flows, *J. Appl. Phys.* **27**, 11, 1323–1328 (1956).
3. P. L. CHAMBRÉ, On chemical surface reactions in hydrodynamic flows, *Appl. Sci. Res.* A **6**, 2–3, 97–113 (1956).
4. A. ACRIVOS and P. L. CHAMBRÉ, Laminar boundary layer flows with surface reactions, *Industr. Engng Chem.* **49**, 6, 1025–1029 (1957).
5. D. E. ROSNER, Chemically frozen boundary layers with catalytic surface reaction, *J. Aero/Space Sci.* **26**, 5, 281–286 (1959).
6. P. M. CHUNG and A. D. ANDERSON, Heat transfer to surfaces of finite catalytic activity in frozen-dissociated hypersonic flow. *NASA* TN D-350 (January 1961).
7. P. M. CHUNG and A. D. ANDERSON, Surface recombination in the frozen compressible flow of a dissociated diatomic gas past a catalytic flat plate *J. Amer. Rocket Soc.* **30**, 3, 263–264 (1960).
8. P. M. CHUNG, S. W. LIU and H. MIRELS, Effect of discontinuity of surface catalycity on boundary layer flow of dissociated gas. TDR-69(2240-20) TN-1. Aerospace Corporation, El Segundo, Calif. (June 1962).
9. M. J. LIGHTHILL, Contributions to the theory of heat transfer through a laminar boundary layer, *Proc. Roy. Soc. London*, A **202**, 359–377 (1950).
10. M. W. RUBESIN and M. INOUYE, A theoretical study of the effect of upstream transpiration cooling on the heat transfer and skin friction characteristics of a compressible laminar boundary layer. *NACA* TN-3969 (May 1957).
11. D. R. CHAPMAN and M. W. RUBESIN, Temperature and velocity profiles in compressible laminar boundary layers with arbitrary distribution of surface temperatures, *J. Aero/Space Sci.* **16**, 547 (1949).
12. L. LEES, Laminar heat transfer over blunt-nosed bodies at hypersonic flight speeds, *Jet Propulsion*, **26**, 4, 259–269 (1956).
13. L. LEES, Convective heat transfer with mass addition and chemical reactions. *Third AGARD Combustion and Propulsion Colloquium*, Palermo, Sicily, pp. 451–498. Pergamon Press, New York (March 1958).
14. F. K. MOORE, On local flat-plate similarity in the hypersonic boundary layer, *J. Aero/Space Sci.* **28**, 10, 753–762 (1961).
15. N. H. KEMP, P. H. ROSE and R. W. DETRA, Laminar heat transfer around blunt bodies in dissociated air, *J. Aero/Space Sci.* **26**, 7, 421–430 (1959).
16. G. R. INGER, Specific heat inequality effect in the chemically frozen stagnation point boundary layer, *J. Amer. Rocket Soc.* **30**, 11, 1028–1029 (1960).
17. R. J. COULARD, On catalytic recombination rates in hypersonic stagnation heat transfer, *Jet Propulsion*, **28**, 11, 737–745 (1958).
18. A. N. TIFFORD and S. T. CHU, Heat transfer in laminar boundary layers subject to surface pressure and temperature distributions. *Proc. Second Midwestern Conf. Fluid Mech.*, pp. 363–377. Ohio State University, Columbus, Ohio (March 1952).
19. L. A. PIPES, *Applied Mathematics for Engineers and Physicists*, First Edition, pp. 277–278 and 5–15. McGraw-Hill, New York (1946).
20. W. J. RAE, An approximate solution for the non-equilibrium boundary layer near the leading edge of a flat plate. I.A.S. National Summer Meeting, Los Los Angeles (June 1962).

Résumé—Cet article étudie plusieurs types nouveaux de solutions exactes, développées en séries, de l'équation de diffusion d'écoulements de couches limites laminaire, dissociée et chimiquement figée autour d'obstacles, avec distribution continue de vitesse de recombinaison atomique du premier ordre le long de la surface.

On considère les écoulements autour de plaques, de dièdres et de cônes. L'analyse étend la théorie de Chambré et Acrivos, valable pour une efficacité catalytique et une température de surface constantes, au cas où le nombre de Damkohler varie comme une puissance de la distance, ou au cas où ce nombre est distribué sous forme polynomiale en puissances positives, entières ou fractionnaires, de la distance. D'ailleurs, en faisant l'hypothèse d'une similitude locale dans le profil de vitesse, les solutions s'appliquent également, avec une bonne précision, à des corps émoussés hautement refroidis en écoulement hypersonique.

Une méthode de résolution approchée est également étudiée, elle donne une forme analytique extrêmement simple des solutions en series exactes à travers le champ complet de l'écoulement, au

moyen d'une extrapolation locale non linéaire du terme principal de la série. Plusieurs exemples montrent que cette technique fournit des résultats très précis en ce qui concerne la concentration atomique, le flux de diffusion, la distribution des échanges thermiques, pour un certain nombre de variations de l'efficacité catalytique de la paroi dans le sens de l'écoulement.

Zusammenfassung—Die Arbeit behandelt verschiedene neue Typen exakter Reihenlösungen der Diffusionsgleichung für chemisch eingefrorene, dissoziierte, laminare Grenzschichtströmungen an Körpen mit beliebiger, kontinuierlicher Verteilung Atomrekombination erster Ordnung entlang der Oberfläche. Platten-, Keil- und Kegelströmungen wurden untersucht. Die Analyse erweitert die Theorie von Chambré und Acrivos für konstante katalytische Oberflächenwirkung und Temperatur auf den Fall, dass sich die Damköhlerzahl der Oberfläche nach Potenzen der Entfernung ändert oder als Polynom ganzer oder gebrochener positiver Potenzen des Abstandes vorliegt. Darüber hinaus lassen sich die Lösungen, die mit der Näherung erzielt wurden, dass für die Geschwindigkeitsprofile örtliche Ähnlichkeit vorliegt, mit guter Genauigkeit auf stark gekühlte stumpfe Körper in Hyperschallströmung anwenden.

Ebenfalls dargestellt wird eine Methode zur näherungsweisen Lösung. Durch lokale nichtlineare Extrapolation des Führungsgliedes der Reihe ermöglicht sie eine extrem einfache, geschlossene Darstellungsform der exakten Reihenlösungen im ganzen Strömungsbereich. Einige Beispiele liefern mit dieser Technik sehr genaue Ergebnisse für die Atomkonzentration an der Oberfläche, den Diffusionsstrom und die Verteilung des Wärmeüberganges für mehrere Variationen der Katalysierwirkung der Wand in Strömungsrichtung.

Аннотация—В данной статье рассматривается несколько новых типов точных решений в виде ряда уравнения диффузии для химически замороженных диссоциированных ламинарных пограничных слоев у тел с произвольным непрерывным распределением скорости рекомбинации первого порядка атомов вдоль поверхности. Приводятся случаи обтекания пластины, клина и конуса. Данные Шабрэ и Акриво для случая постоянной каталитической эффективности и температуры поверхности используются для случая, когда число Дамкелера на поверхности изменяется как любая степень расстояния или как любой полином, содержащий целые или дробные (положительные) степени расстояния. Кроме того, путем использования приближения локального подобия в профиле скорости полученные решения можно с хорошей точностью применять также к интенсивно охлажденным тупым телам в сверхзвуковом потоке.

Разработан также приближенный метод решения, который дает возможность с помощью локальной нелинейной экстраполяции главного члена ряда получить по всему полю течения чрезвычайно простые представления в замкнутой форме точных решений в виде рядов. Имеется ряд подтверждений того, что данная техника расчета дает очень точные результаты при определении концентрации атомов у поверхности, плотности диффузионного потока и распределения переноса тепла при различном изменении вдоль потока каталитической активности стенки.